

Similar oxysterols may lead to opposite effects on synaptic transmission: Olesoxime versus 5 α -cholestan-3-one at the frog neuromuscular junction



M.R. Kasimov, G.F. Zakyrganova, A.R. Giniatullin, A.L. Zefirov, A.M. Petrov*

Department of Normal Physiology, Kazan State Medical University, Kazan 420012, Russia

ARTICLE INFO

Article history:

Received 18 December 2015

Received in revised form 17 March 2016

Accepted 15 April 2016

Available online 18 April 2016

Keywords:

Olesoxime

5 α -Cholestan-3-one

Synaptic vesicle cycle

Neuromuscular junction

Neurotransmitter release

ABSTRACT

Cholesterol oxidation products frequently have a high biological activity. In the present study, we have used microelectrode recording of end plate currents and FM-based optical detection of synaptic vesicle exo-endocytosis to investigate the effects of two structurally similar oxysterols, olesoxime (cholest-4-en-3-one, oxime) and 5 α -cholestan-3-one (5 α Ch3), on neurotransmission at the frog neuromuscular junction. Olesoxime is an exogenous, potentially neuroprotective, substance and 5 α Ch3 is an intermediate product in cholesterol metabolism, which is elevated in the case of cerebrotendinous xanthomatosis. We found that olesoxime slightly increased evoked neurotransmitter release in response to a single stimulus and significantly reduced synaptic depression during high frequency activity. The last effect was due to an increase in both the number of synaptic vesicles involved in exo-endocytosis and the rate of synaptic vesicle recycling. In contrast, 5 α Ch3 reduced evoked neurotransmitter release during the low- and high frequency synaptic activities. The depressant action of 5 α Ch3 was associated with a reduction in the number of synaptic vesicles participating in exo- and endocytosis during high frequency stimulation, without a change in rate of the synaptic vesicle recycling. Of note, olesoxime increased the staining of synaptic membranes with the B-subunit of cholera toxin and the formation of fluorescent ganglioside GM1 clusters, and decreased the fluorescence of 22-NBD-cholesterol, while 5 α Ch3 had the opposite effects, suggesting that the two oxysterols have different effects on lipid raft stability. Taken together, these data show that these two structurally similar oxysterols induce marked different changes in neuromuscular transmission which are related with the alteration in synaptic vesicle cycle.

© 2016 Elsevier B.V. All rights reserved.

1. Introduction

Chemical synaptic transmission results from the release from the nerve terminal of neurotransmitter that is packaged in synaptic vesicles. During neurotransmission, synaptic vesicles fuse at the active zone and their membranes become incorporated into the presynaptic membrane. These vesicle components must be captured by endocytosis to maintain the number of vesicles and the molecular identity of the presynaptic membrane. The newly formed vesicles are then filled with neurotransmitter and transported to the vesicle pool. Thus, as a consequence of synaptic activity, vesicles undergo a membrane-trafficking cycle in the nerve terminals [1]. This synaptic cycle is a tightly regulated process which is closely influenced by the availability of cholesterol. Cholesterol depletion may alter the balance between evoked and spontaneous

exocytosis, and the distribution of proteins and ion channels involved in exocytosis. It may also lead to severe disturbances of endocytosis [2–8]. Neuronal membrane cholesterol has a very long half-life and can be oxidized by specific enzymes and reactive oxygen species [9, 10]. In addition, oxidized cholesterol-like molecules produced in extraneuronal tissues can act on neurons. Some forms of oxysterol show high biological activity such as regulating cell survival and apoptosis [9, 11]. Recent studies indicate that 24(S)-hydroxycholesterol may function as an endogenous modulator of NMDA receptors in the hippocampus [12] and enzymatic cholesterol oxidation can influence on synaptic vesicle cycle at the frog neuromuscular junction [13]. However, the details of how these cholesterol derivatives influence synaptic transmission are still poorly understood.

Recently, we have reported that 5 α -cholestan-3-one (5 α Ch3), in low concentration (0.2 μ M), reduces the number of vesicles which are actively recruited during synaptic transmission and alters membrane properties at the mouse neuromuscular junction [14]. The production of this oxysterol is up-regulated in the rare genetic disease, cerebrotendinous xanthomatosis, which is associated with central-peripheral distal axonopathy. The level of 5 α Ch3 in the blood from sterol 27-hydroxylase gene-deficient mice (model of cerebrotendinous

Abbreviations: α -Btx, α -bungarotoxin; 5 α Ch3, 5 α -cholestan-3-one; bodipy-ganglioside GM1, BODIPY® FL C5-ganglioside GM1; MEPC, miniature postsynaptic end-plate currents; EPC, postsynaptic end-plate current; 22-NBD-cholesterol, 22-(N-(7-nitrobenz-2-oxa-1,3-diazol-4-yl)amino)-23,24-bisnor-5-cholestan-3 β -ol; CTxB, subunit B from cholera toxin.

* Corresponding author at: Kazan, Butlerova st. 49, Kazan State Medical University, Department of Normal Physiology, 420012, Russia.

E-mail address: fysio@rambler.ru (A.M. Petrov).

xanthomatosis) is about 0.2 μM [15]. On the other hand a structurally related compound, olesoxime (cholest-4-en-3-one, oxime), has beneficial effects in disease models of amyotrophic lateral sclerosis, peripheral neuropathies and neurodegenerative pathologies. Recently, clinical trials (phases II and III) have shown that treatment with olesoxime was associated with maintenance of motor function and decrease in frequency of complications in patients with spinal muscle atrophy [16]. Note that olesoxime shows the potent protective properties in the submicromolar range [11,17–19]. However, nothing is known about the influence of olesoxime on synaptic transmission. In the current study we have investigated how two similar oxysterols (olesoxime and 5 α -cholestan-3-one) change neurotransmitter release and the synaptic vesicle cycle at the frog neuromuscular junction.

2. Material and methods

2.1. Ethical approval

The investigation was performed in accordance with the Guide for the Care and Use of Laboratory Animals published by the US National Institutes of Health (NIH publication no. 85-23, revised 1996). Frogs (*Rana ridibunda*) were collected from lakes during early autumn, and were kept in the dark at 4 °C in a humidity- and temperature-controlled environment. Frogs were provided with a pool of dechlorinated flowing water. Experiments were carried out in the autumn–winter period. Frogs were killed by decapitation and destruction of the brain and the spinal cord, and then the muscles were quickly excised. All efforts were made to minimize suffering. The experimental protocol met the requirements of the European Communities Council Directive 86/609/EEC and was approved by the Ethical Committee of Kazan Medical University.

2.2. Solution and chemicals

Isolated cutaneous pectoris muscles with a nerve were pinned to the bottom of a glass chamber lined with Sylgard, and were superfused during the experiment with frog Ringer's saline containing (in mM): NaCl – 113.0, KCl – 2.5, CaCl₂ – 1.8, and NaHCO₃ – 2.4. pH was adjusted to 7.3 with NaOH/HCl and the temperature was kept at 23–24 °C. The muscle fibers (MF) were cut transversely to prevent muscle contractions while maintaining the physiological level of quantal release of acetylcholine at the neuromuscular junction [20]. Experiments were started after washing the muscle for 40 min with Ringer's solution. 5 α Ch3 and olesoxime were dissolved in DMSO (dimethylsulfoxide) such that the final concentration of DMSO in the working solution did not exceed 0.001%. In concentration 0.001% DMSO in bathing solution did not change the parameters of both evoked and spontaneous postsynaptic signals, labelings with FM1–43 dye and membrane-markers used here. We therefore used these data as the additional control.

Applications of 5 α Ch3 (200 nM) or olesoxime (200 nM) lasted 20 min. After the treatments, these reagents were washed out for 10 min. The concentration was chosen based on (1) our previous study, where 5 α Ch3 in this concentration had profound presynaptic effects [14], (2) data about the level of 5 α Ch3 in the blood from the mice with disrupted sterol 27-hydroxylase gene [15] and (3) observations that olesoxime could effectively protect cells from oxidative stress and death even in the submicromolar range [11,17,18]. The incubation period was 20 min because this time is necessary for the changes in postsynaptic currents, induced by these drugs, to reach a steady state level.

All reagents were from Sigma, except for fluorescent dyes, which were purchased from Molecular Probes.

2.3. Electrophysiology

Recording of the postsynaptic end-plate currents (EPCs) and miniature EPC (MEPCs) was performed using standard two-electrode voltage

clamp technique with intracellular glass microelectrodes (tip diameter ~ 1 μm , resistance 3–5 M Ω , filled with 2.5 M KCl). The synaptic zone was located between two electrodes separated by a distance of ~200–300 μm . The holding potential for the cut MFs was kept at –40 mV (leak current in the range of 10–30 nA, \leq 10% of EPC amplitudes). EPCs were elicited by supra-threshold stimulation (0.1 ms duration) of the motor nerve via a suction electrode connected to an extracellular stimulator (DS3 Digitimer Ltd., UK). The motor nerve was stimulated by a single stimulus (1 stimulus in 20 s, 0.05 Hz) or by high-frequency trains (20 stimuli per 1 s, 20 Hz, for 3 min). The recorded signals were digitized at 50 kHz and analyzed off-line using PC software [3]. No changes in the muscle cable properties occur after cutting the muscle fibers and the voltage clamp technique enables long-lasting stable recording of postsynaptic currents [21]. Recording instrumentation consisted of an Axoclamp 900 A (Molecular devices, USA) amplifier and LA II digital I/O board (Pushchino, Russia) under the control of locally written software.

2.4. Fluorescence microscopy

An Olympus BX51WI microscope with a confocal Disk Speed Unit attachment and a focus stepper (for multiple z axis optical sections; ECO-MOT, Marzhauser Wetzlar GmbH & Co. KG, Germany) were used for image acquisition. Images were captured with UPLANSapo 60xw or LumPlanPF 100xw objectives and an Orca R2 (Hamamatsu, UK) CCD camera under control of Cell^P (Olympus) software. Image analysis in regions of interest was performed using ImagePro software (Media Cybernetics, Bethesda, MD, USA) and the fluorescence was calculated in arbitrary unit (a.u.), and in some cases then converted to percentages. Only surface-lying nerve terminals were studied.

2.4.1. Loading and unloading of FM1–43

The fluorescent probe FM1–43 (3 μM , Molecular Probes) was used for imaging of synaptic vesicle exo- and endocytosis [22]. To load the dye into the nerve terminals, we electrically stimulated the nerve for 3 min at 20 Hz. The FM1–43 was in the bath during the stimulation period and for 7 min afterwards. The muscles were then perfused for at least 30 min with dye-free physiological saline with ADVASEP-7 (3 μM , Sigma) to decrease background fluorescence [23]. Electrical stimulation of the nerve at 20 Hz evoked unloading of the dye (due to synaptic vesicle exocytosis) from the pre-loaded nerve terminals. To estimate the impact on endocytosis, the muscles were exposed to 5 α Ch3 or olesoxime before dye loading. The oxysterols were added after washing with ADVASEP-7 but prior to the start of the unloading stimulation.

The dye FM2–10 (24 μM , Molecular Probes) was used to label synaptic vesicles in the recycling pool. The motor nerves were stimulated at 2 Hz for 5 min in the presence of FM2–10, the muscles were then washed in normal physiological saline with ADVASEP-7 for the first 30 min and with oxysterol (or without in the control) for the next 20 min. After this unloading was performed using 2 Hz stimulation.

The dye FM1–43 (or FM2–10) was excited by light of 480/10 nm wavelength and was recorded using a 515–555 nm band pass emission filter. Nerve terminal fluorescence was defined as the mean intensity per pixel in the regions of interest after subtracting background FM-fluorescence, measured in a 20 μm^2 area outside of the nerve terminal [23]. For plotting of the dye-unloading curves, values of the initial nerve terminal fluorescence (a.u. before the stimulation) were set to 1.0.

2.4.2. Labeling of lipid rafts

Ganglioside GM1, a well-established lipid raft component, was visualized using Alexa Fluor 488-labeled cholera toxin subunit B (CTxB) (Molecular Probes), which is pentavalent for ganglioside GM1 and preferentially interacts with GM1-molecules from lipid rafts [24]. The muscles were exposed to CTxB (1 $\mu\text{g}/\text{ml}$, diluted in Ringer's saline) for 15 min at 23–24 °C and were then perfused for 30 min prior to image

capturing. The oxysterols were added before the CTxB staining procedure. CTxB fluorescence was detected using a 480/15 nm wavelength light and a 505–545 nm band-pass filters. The fluorescence was calculated as the average fluorescence from all the pixels in junctional membrane regions [14].

2.4.3. Staining with fluorescent ganglioside GM1

For direct indication of the distribution of ganglioside GM1 in the plasma membranes, an exogenous green-fluorescent BODIPY® FL C5-ganglioside GM1 (bodipy-ganglioside GM1) complexed to bovine serum albumin (Molecular Probes) was used [25]. Bodipy-ganglioside GM1 was diluted in physiological solution (final concentration 0.1 μM) and incorporated into living preparations by incubation for 20 min at 23–24 °C. Additional washing step for 30 min was applied to remove unbound fluorescent ganglioside GM1. Superficial synaptic regions of the muscle were imaged (using a light of 480/10 nm wavelength for excitation and a band-pass 500–550 nm emission filter) in the control and during exposure to oxysterols. The fluorescence was calculated as average brightness of all pixels of nerve terminal outline or of selected spots within the terminal.

2.4.4. Staining with fluorescent labeled sterol

In addition, labeling of surface membrane with fluorescent sterols was used. 22-NBD-cholesterol (22-(N-(7-Nitrobenz-2-Oxa-1,3-Diazol-4-yl)Amino)-23,24-Bisnor-5-Cholen-3 β -Ol, Molecular Probes) was applied as an environment-sensitive probe that localizes in the membrane's interior [26,27]. 22-NBD-cholesterol fluorescence was excited at 480/15 nm wavelength and emission was reordered using a band-pass filter of 510–590 nm. 22-NBD-cholesterol was dissolved in pure ethanol 10 mg/0.1 ml to obtain final concentration 0.2 μM in physiological saline where the muscles were incubated for 20 min at 23–24 °C followed by a 30 min wash. Afterwards the time course of 22-NBD-cholesterol fluorescence was detected at the synaptic region in the control and during application of olesoxime or 5 α Ch3.

2.4.5. Rhodamine-conjugated α -bungarotoxin labeling

Additional staining with rhodamine-conjugated α -bungarotoxin (100 ng/ml α Btx, Molecular Probes), a specific marker of postsynaptic acetylcholine receptors, helped to identify the synaptic region for detection of CTxB, bodipy-ganglioside GM1 or 22-NBD-cholesterol fluorescence. α Btx was added to the external solution simultaneously with CTxB, bodipy-ganglioside GM1 or 22-NBD-cholesterol. Fluorescence of α Btx was excited by light of 555/15 nm wavelength and emission was detected using a band-pass filter of 610–650 nm.

2.4.6. Immunolabeling

Prior to immunofluorescent staining, all (control, olesoxime and 5 α Ch3 pre-treated) neuromuscular preparations were fixed with 3.7% p-formaldehyde for 20 min at room temperature. The immunofluorescent labeling protocol was described in details here [14]. Primary polyclonal antibodies, rabbit anti-syntaxin antibody (at dilution 1:200, Abcam) and goat anti-synaptophysin antibody (at dilution 1:200, Santa Cruz Biotechnology) were used for immunolabeling of isolated neuromuscular preparations. The localization of the primary antibodies was determined using the following secondary fluorescent-labeled antibodies (at dilution 1:1000, Abcam): donkey anti-rabbit antibody conjugated to Alexa Fluor 647 to detect anti-syntaxin antibodies and donkey anti-goat antibodies conjugated to Alexa Fluor 488 to detect anti-synaptophysin antibodies. No fluorescent staining was detected if primary or secondary antibodies were not added. In addition immunostainings were not observed after pre-incubations of each primary antibody with the respective peptide immunogen (rat syntaxin 1a peptide ab41452, Abcam; sc-7568 P, Santa Cruz Biotechnology).

2.5. Statistics

Statistical analysis was performed using Origin Pro software (OriginLab Corp.). Data are presented as mean \pm SEM, where n is the number of independent experiments (different animals), with statistical significance assessed by Student's t test or ANOVA. Values of $p < 0.05$ were considered significant. For CTxB and FM1–43 loading experiments, we used 9–12 neuromuscular junctions to estimate means and SEMs and number of animals (seven to eight) as a sample size (n) for statistical comparisons.

3. Results

3.1. Olesoxime potentiates and 5 α Ch3 depresses transmitter release during rhythmic synaptic activity

To test the impact of oxysterols on spontaneous release, MEPCs were initially recorded under control conditions and then after 20 min exposure to oxysterols (Fig. 1). In olesoxime (n = 6 animals) and 5 α Ch3 (n = 6 animals) treated neuromuscular junctions the MEPC amplitudes were not changed compared to control ($p > 0.05$ paired t-test) (Fig. 1A, B). These oxysterols had a negligible influence on MEPC frequency (initial value $1.36 \pm 0.14 \text{ s}^{-1}$, n = 12 animals) (Fig. 1B), a sign of spontaneous quantal release. Olesoxime did not significantly modify (n = 6 animals, $p = 0.064$ paired t-test), while 5 α Ch3 slightly increased the MEPC frequency (by $7 \pm 3\%$, n = 6 animals, $p = 0.037$ paired t-test). This indicates that, in contrast to olesoxime, 5 α Ch3 has little stimulatory action on spontaneous release.

In conditions of low-frequency activity (0.05 Hz), treatments with olesoxime lead to slight increase of the EPC amplitude to $112 \pm 4\%$ (n = 6 animals, $p < 0.05$), but application of 5 α Ch3 decreased the EPC amplitude to $71 \pm 5\%$ (n = 6 animals, $p < 0.05$) (Fig. 2A, B). The effects of both oxysterols were observed after 8–10 min of application, reached a plateau by 16–20 min and then remained at this level for at least 1 h. Since the MEPC amplitudes were constant, the observed changes in EPC amplitudes indicate an enhancement or reduction of the evoked exocytotic events in response to a single stimulus owing to the action of olesoxime or 5 α Ch3, respectively.

At the frog neuromuscular junction, which contains a relatively large population of docked synaptic vesicles, the low-frequency activity should recruit only vesicles belonging to the readily releasable pool [28]. In contrast, during high-frequency stimulation, the efficiency of neurotransmitter release is tightly dependent on the delivery of undocked synaptic vesicles to the active zones and to vesicle recycling

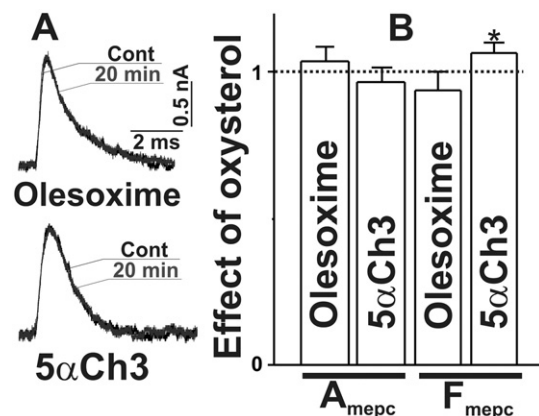


Fig. 1. The oxysterols and spontaneous postsynaptic events. A. Typical MEPCs prior to and 20 min after treatment with olesoxime or 5 α Ch3. B. Histograms pointing the influence of olesoxime and 5 α Ch3 on peak MEPC amplitude (A_{mepc}) and MEPC frequency (F_{mepc}). 5 α Ch3 slightly increases spontaneous neurotransmitter release, while olesoxime has no any influence. Means \pm SEM. Y-axis shows the normalized effect of oxysterol (1.0 – is the value before the oxysterol application).

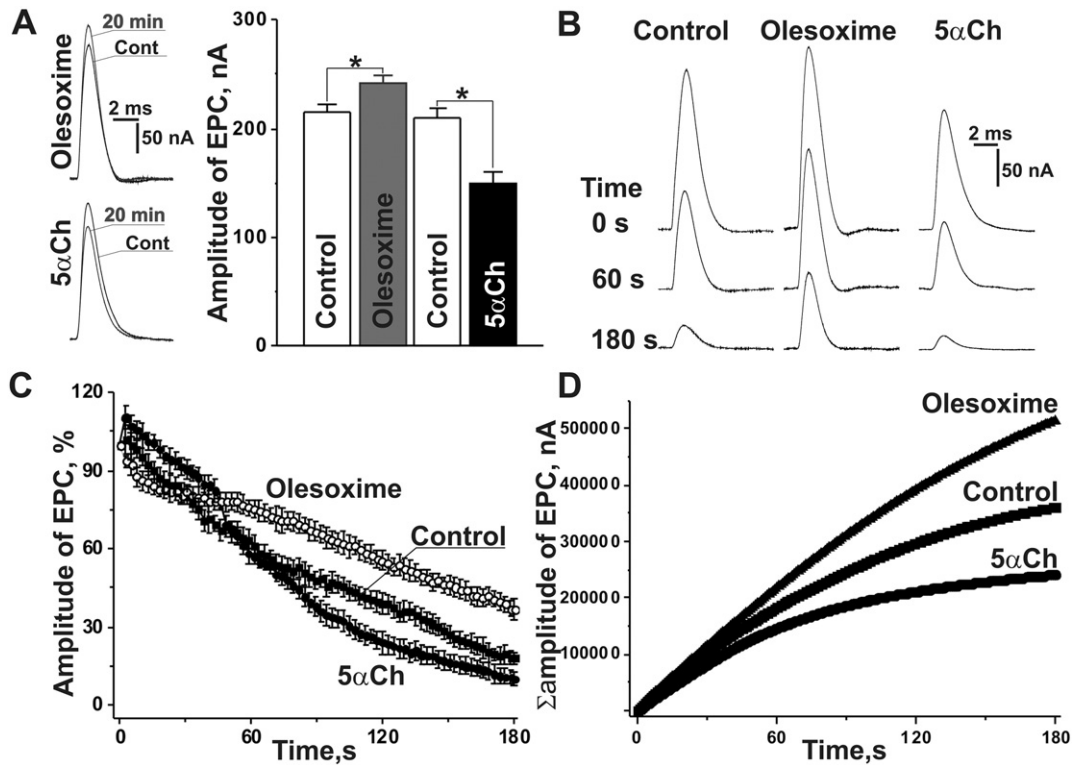


Fig. 2. Influence of the oxysterols on evoked neurotransmitter release. A. Representative EPC (native signals and amplitude) in response to a single stimulus before and 20 min after treatment with oxysterol, olesoxime or 5αCh3. Olesoxime increases, while 5αCh3 increases the EPC. Histogram showing the opposite actions of olesoxime and 5αCh3 on EPC amplitude. Means \pm SEM. Asterisks denote significant differences ($*p < 0.05$). B. Typical EPCs at 0, 1 and 3 min of high-frequency stimulation in the control and in the presence of olesoxime or 5αCh3. C. The time-course of the EPC amplitudes during high-frequency stimulation for 3 min in the control and in oxysterol-treated muscles. Means \pm SEM. D. Cumulative curves of the EPC amplitudes (from C) at high-frequency activity. D–C. Panels indicate the strengthening and depressant effect of olesoxime and 5αCh3, respectively, on the EPC amplitudes during 3 min 20 Hz-stimulus train.

[22,29]. High-frequency stimulus trains resulted in a change in the EPC amplitude (Fig. 2B, C). Within the first few seconds the amplitude transiently increased, and then for the remaining period of stimulation it declined with a relatively constant rate to about $61 \pm 4\%$ and $18 \pm 3\%$ of the pre-stimulation value ($n = 6$ animals, $p < 0.01$ versus baseline) after 1 and 3 min of stimulation, respectively.

After olesoxime-pretreatment the initial facilitation was less profound, but the following depression of the EPC amplitude occurred more slowly (Fig. 2B, C). After 1 min of stimulation the EPC amplitude decreased only to $75 \pm 3\%$ ($n = 6$ animals, $p < 0.05$ compared to the control curve). For 3 min of stimulation, the EPC amplitude was reduced to $37 \pm 4\%$ ($p < 0.001$, compared to the control curve). Treatment with 5αCh3 influences the EPC dynamics in two opposite ways. During the first seconds of stimulation a more pronounced potentiation of the EPC amplitude was observed, but 30–40 s later the EPC amplitude started to fall at a higher rate than in the control (Fig. 2B, C). Therefore 1 and 3 min of stimulation caused a significant decline of the EPC amplitude to $58 \pm 3\%$ ($n = 6$ animals, $p > 0.05$ versus control) and $10 \pm 3\%$ ($p < 0.05$, versus control), respectively. Summation of the EPC amplitudes during rhythmic activity allowed us to estimate the total number of transmitter quanta released, both in the control and under the influence of drugs (Fig. 2D). The cumulative EPC amplitude was significantly increased (to $\sim 142\%$ of the control value, $p < 0.01$) or reduced (to $\sim 67\%$ of the control value, $p < 0.01$) after 3 min of stimulation in olesoxime or 5αCh3-treated preparations.

In addition, 5αCh3, but not olesoxime, interfered with recovery of the EPC amplitude after high frequency stimulation (data not shown). We observed a full recovery of the EPC amplitude after 3–4 min in both control and olesoxime pretreated muscles. However, in 5αCh3-pretreated preparations, the EPC amplitude did not recover completely and was maintained at 65–80% of the pre-stimulation baseline ($n = 5$

animals, $p < 0.01$ versus control). This may indicate a lack of fusion competence of synaptic vesicles newly formed by endocytosis.

3.2. Olesoxime increases and 5αCh3 decreases FM1–43 loading induced by high-frequency stimulation

Nerve terminals were loaded with FM1–43 by 20 Hz stimulus trains lasting 3 min (Fig. 3). The mean fluorescence of spots after loading in the control conditions was 122 ± 6 a.u. ($n = 8$ animals, 82 muscle fibers). The mean spot fluorescence in olesoxime was 154 ± 8 a.u. ($n = 8$ animals, 85 muscle fibers, $p < 0.05$ versus control) and in 5αCh3 was 91 ± 7 a.u. ($n = 8$ animals, 84 muscle fibers, $p < 0.05$ versus control). In other words, the nerve terminals of olesoxime or 5αCh3-pretreated muscles captured 25% more or less dye than controls during 3 min stimulation, respectively. Note that olesoxime caused a greater increase in neurotransmitter release than in FM1–43 uptake (Fig. 2D versus Fig. 3C). One possible reason for this is an increase in the number of synaptic vesicles which participate repeatedly in recycling during stimulation (3 min, 20 Hz), causing an underestimate of synaptic vesicle endocytosis [22,23].

Since both olesoxime and 5αCh3 are derivatives of cholesterol, control experiments were performed in order to test the effects of these drugs on both the fluorescence from superficial membrane-bound FM1–43 (in green and red channels) and washing the dye out from the plasma membranes of neuromuscular junctions (Suppl. Fig. 1A, B). It was observed that neither of the two drugs interferes with the properties of FM1–43.

3.3. Olesoxime accelerates and 5αCh3 slows FM1–43 unloading

The nerve stimulation of FM1–43 preloaded muscles led to a decrease in FM1–43 fluorescence in nerve terminals (Fig. 4), pointing to

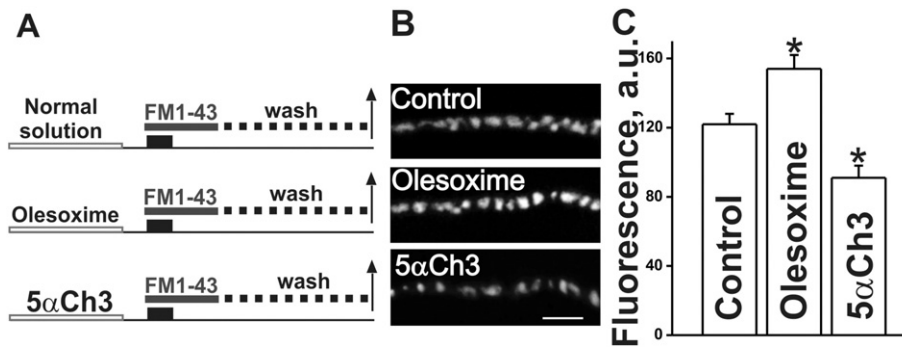


Fig. 3. Opposite effects of the oxysterols on dye FM1–43 loading. **A.** Protocols of the experiments. After exposure to Ringer solution without or with oxysterols, the muscles were loaded with FM1–43 by 20 Hz-stimulation of the motor nerve for 3 min. **B.** The fluorescent images of the nerve terminals loaded with FM1–43. Scale bar – 5 μm. **C.** Intensities of FM1–43 fluorescence in the control and the oxysterol treated neuromuscular junctions. Means ± SEM. Asterisks denote significant differences (**p* < 0.05). **B, C.** Panels demonstrate that olesoxime increases whereas 5αCh3 decreases the FM1–43 fluorescence.

the rate of exocytosis of FM-labeled synaptic vesicles. In the control conditions (Fig. 4Aa), after 1 min and 3 min of 20 Hz-stimulation, the fluorescence decreased to $80.5 \pm 2.0\%$ (*n* = 8 animals, *p* < 0.01

relatively baseline) and $66.3 \pm 3.1\%$ (*p* < 0.001) of the baseline value, respectively (Fig. 4Ca; Ea). Olesoxime-treatment of muscles preloaded with FM1–43 accelerated the FM1–43 unloading induced by

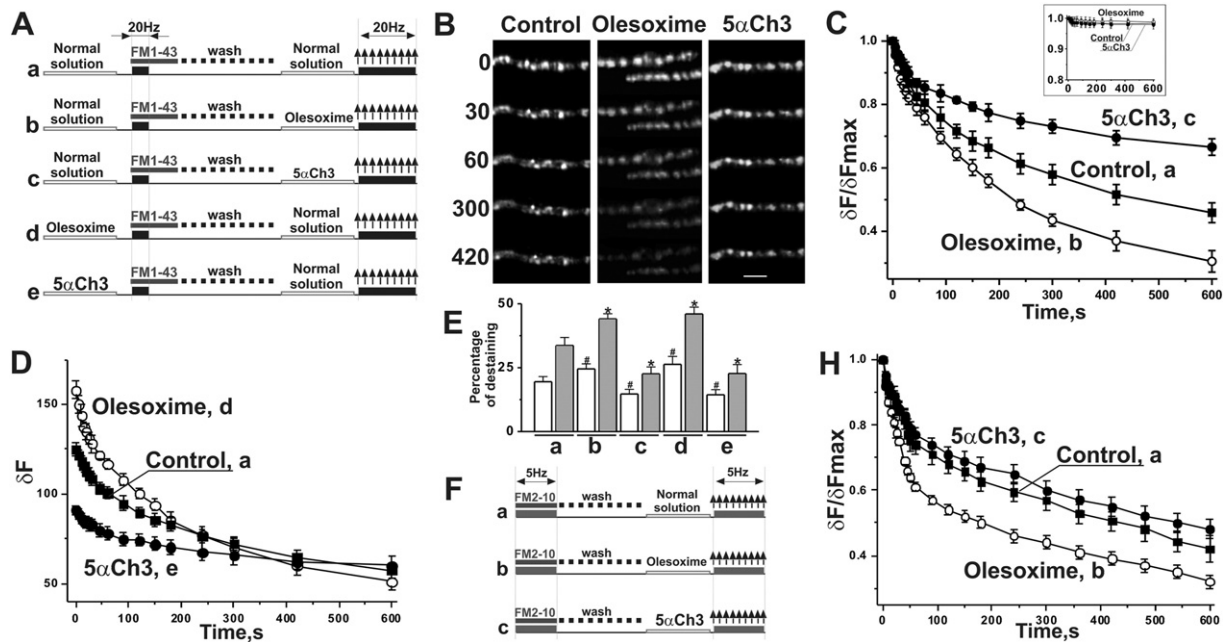


Fig. 4. Effects of the oxysterol on time-course of FM-unloading. **A.** Design of the experiments for which the results are presented in **B, C, D** and **E.** To load FM1–43 dye, motor nerve was stimulated by 20 Hz for 3 min (1st black column). The dye was presented in the bath solution (upper gray line) during stimulation and 5 min after. Owing to this loading protocol, in frog neuromuscular junctions the FM dye is uptaken into the synaptic vesicles from both recycling and reserve pools. To decrease non-specific fluorescence the muscles were then washed with physiological saline with ADVASEP-7 (this reagent facilitates dissociation of FM1–43 from the membranes) for 30 min (upper dotted line). After the washout period the muscles were treated with normal or oxysterol-containing solution (2nd light column) and then were re-stimulated (20 Hz, 2nd black column) under condition of intense perfusion by dye-free solution. The nerve terminal images were captured (arrows) to detect a decrease in the fluorescence due to loss of the dye during exocytosis of stained synaptic vesicles (unloading). An initial segment of dye unloading curve shows exocytosis of the vesicles belonging to recycling pool, while ~30 s after the onset of stimulation the reserve pool vesicles mainly participate in the dye release. In some experiments (the last two schemes) the muscles were exposed to the oxysterols (1st light column) prior to loadings. Under these conditions the FM1–43 loadings are modified due to the oxysterol action and sequential unloading stimulation helps to estimate the fusion-competence of newly formed synaptic vesicles. **B.** The fluorescent images of segments of the nerve terminals immediately prior to 20 Hz stimulation (0) and at different times (in s) during the stimulation. Scale – 5 μm. After the onset of stimulus train, the fluorescence decreases with different rates in the control (a) and oxysterol-treated neuromuscular junctions (b, c). **C.** Unloading curves determined in the preparation treated with the olesoxime (b) and 5αCh3 (c) after FM1–43 loading. These curves show that olesoxime increases the rate of FM1–43 unloading throughout the 20 Hz stimulation, while 5αCh3 markedly suppresses the unloading starting from 40 s of the stimulus train. Inset shows the FM1–43 photobleaching curves in the control and in the presence of the oxysterol. The illumination of the FM1–43 stained nerve terminals (without any stimulation) results in almost no change in the fluorescence intensity in all groups. **D.** The destaining kinetics in the muscles which were initially exposed to the oxysterols and then loaded with FM1–43 (d, e). Under these conditions, the initial fluorescence (in a.u.) was higher (olesoxime) or lower (5αCh3) than in the control. Despite this, unloading from olesoxime or 5αCh3-treated nerve terminals occurs faster or slower versus control, respectively. It indicates long lasting effects of the oxysterol on exocytosis-competence of synaptic vesicle during high-frequency stimulation. **E.** Bar graphs showing average percentage of FM1–43 destaining (Y-axis) of control (a) and oxysterol-treated (b, c, d, e) neuromuscular junctions 1 min (light bar) and 3 (gray bar) min after stimulation. Asterisks denote significant differences versus percentage of destaining in the control (a) due to 1 min (**p* < 0.05) or 3 min (**p* < 0.05) stimulation. **F.** The protocols that were used to describe exocytosis of synaptic vesicles that selectively populate the recycling pool (outcomes are in **H**). A 2 Hz stimulation for 5 min (1st gray column) was used for loading of vesicle from the recycling pool. FM2–10 was presented in the bath solution only during the 1st stimulus train. FM2–10 unloading was evoked by a second 2 Hz stimulation (2nd gray column) following treatment with oxysterol. Other details are as in **A**. **H.** The rate of FM2–10 fluorescence loss during continuous 2 Hz stimulation. Under these conditions olesoxime still enhances the rate of FM2–10 unloading, while 5αCh3 does not modify the FM2–10 unloading curve significantly. The last indicates failure in the ability of the 5αCh3 to impact markedly on the involvement of the vesicle from recycling pool in neurotransmission. On the Y-axis – the relative fluorescence intensity ($\delta F/F_{\max}$), where 1.0 represents the fluorescence before the high-frequency stimulation (**C, H**); the absolute fluorescence (δF) in a.u. (**D**).

subsequent 20 Hz stimulation (Fig. 4Ab, Cb), while exposure to 5 α Ch3 slowed the rate of FM1–43 destaining during the 20 Hz tetanus (Fig. 4Ac; Cc). In the olesoxime-treated muscles, after 1 min and 3 min of the stimulation, the fluorescence decreased to $75.5 \pm 2.0\%$ and to $55.9 \pm 2.0\%$ ($n = 8$ animals, $p < 0.05$ relative to the control curve) respectively (Fig. 4Eb). Under the conditions of 5 α Ch3 administration, the FM1–43 fluorescence was reduced to $85.3 \pm 1.8\%$ and $77.4 \pm 2.7\%$ ($n = 8$ animals, $p < 0.05$ relative to the control curve) after 1 min and 3 min of 20 Hz stimulation, respectively (Fig. 4Ec). Accordingly, in olesoxime or 5 α Ch3-treated preparations, the FM1–43 destaining during 3 min of stimulation was about 17% more or 16% less than in the control. These values are markedly lower than we observed for the cumulative EPC amplitudes (Fig. 2D). Such a difference could be explained by a different number of the synaptic vesicles being repeatedly involved in neurotransmitter release during 3 min of stimulation in the control and oxysterol-pretreated preparations [23,29]. Possibly, after exposure to olesoxime or 5 α Ch3, more or less synaptic vesicles repeatedly participated in synaptic transmission during high frequency stimulation. It should be noted that the oxysterols were added after FM1–43 loading and that the intensity and area of the fluorescence spots were stable during the 20-min exposure to oxysterol, indicating that the agents do not significantly influence FM-dye destaining from resting nerve terminals (Supl. Fig. 1C), for example by influencing spontaneous exocytosis. In addition, to exclude the influence of changes in FM-dye photostability on the unloading, the time course of FM1–43 fluorescence was detected at the same conditions of illumination as when the preparations were stimulated to unload FM1–43. Photobleaching did not significantly occur on the time scale of the stimulus train used for FM1–43 unloading in the presence and absence of olesoxime or 5 α Ch3 (Fig. 4C, inset; the curves were plotted, $n = 4$ animals for each curve).

In some experiments nerve terminals were first treated with olesoxime or 5 α Ch3 and then loaded with FM1–43 and re-stimulated after 30 min washout (Fig. 4Ad, e). In these cases, the initial FM1–43 fluorescence was significantly more (after exposure to olesoxime) or less (after exposure to 5 α Ch3) than in the control conditions (see Section 3.2 section), but the rates of unloading were the same as in the preparations which were treated with oxysterols after FM1–43 loading. In Fig. 4D data are presented in the absolute units to illustrate differences in the initial FM1–43 loadings. In olesoxime-pretreated muscles, the fluorescence decreased to 73.7 ± 3.1 ($n = 8$ animals, $*p > 0.05$ versus muscles exposed to olesoxime after loading) and $54.0 \pm 2.7\%$ ($*p > 0.05$) after 1 min and 3 min of stimulation, respectively (Fig. 4Ed). In 5 α Ch3-pretreated muscles, the fluorescence was reduced to 85.6 ± 2.0 ($n = 8$ animals, $#p > 0.05$ versus muscles exposed to 5 α Ch3 after loading) and $77.3 \pm 3.5\%$ ($#p > 0.05$) after 1 min and 3 min of stimulation, respectively (Fig. 4Ee). It is possible that once applied, the oxysterols have a long-term effect on synaptic vesicle exocytosis and recycling. In addition, data from Fig. 4D indicate that newly formed synaptic vesicles (following treatment with oxysterols) are able to participate in subsequent rounds of fusion.

Differences between the rates of FM1–43 unloading are not clearly expressed within the first minute of 20 Hz-stimulation. At this time, the recycling pool of synaptic vesicles participates intensively in the exocytotic events. To load selectively synaptic vesicles in the recycling pool, we used 2 Hz-stimulation for 5 min in the presence of the less hydrophobic dye, FM2–10 [30]. The muscles were then exposed to normal physiological solution or to the oxysterol and re-stimulated at 2 Hz (Fig. 4F). Olesoxime significantly increased the rate of FM2–10 unloading (Fig. 4H) and after 5 min of 2 Hz stimulation the fluorescence decreased to $44.0 \pm 2.1\%$ of the initial value ($n = 7$ animals, $p < 0.05$ versus control value – $56.9 \pm 3.0\%$, $n = 7$ animals). 5 α Ch3 had no significant influence on the unloading rate (Fig. 4H) and 5 min after starting the 2 Hz stimulation the fluorescence fell to $60.2 \pm 3.1\%$ of the pre-stimulation baseline ($n = 7$ animals, $p > 0.05$ versus control). This indicates that olesoxime, but not 5 α Ch3 has a marked effect on the exocytosis of synaptic vesicle that depends on the recycling pool.

3.4. Olesoxime rises and 5 α Ch3 does not change the recycling of synaptic vesicles

Dye unloading curves indicate the number of synaptic vesicles that released FM dye by exocytosis. After exocytosis, both the dye and neurotransmitter escaped from nerve terminals, and newly formed vesicles contain little or no FM dye. Exocytosis of such vesicles during continued stimulation will produce neurotransmitter release without decrease in FM dye fluorescence. The cumulative EPC amplitude curves show the quantity of neurotransmitter released by exocytosis. Accordingly, superposition of the scaled inverted dye-loss curve and the cumulative EPC amplitude curve allows us to estimate the average time of recycling [22,23,29]. This time (t_r) is defined by the point of evident divergence of the curves, i.e. when the rate of FM unloading starts to lag compared to the rate of neurotransmitter release (Fig. 5). In olesoxime- or 5 α Ch3-treated neuromuscular junctions, divergence of the curves was observed after 25–30 or 50–60 s of stimulation (for comparison, the control value is 50–60 s). This indicates that there is a change in the recycling time in olesoxime treatment, when it is reduced to half its control value, but not in 5 α Ch3.

3.5. Olesoxime and 5 α Ch3 have opposite effects on the properties of synaptic membranes

3.5.1. Staining with CTxB

Several studies have shown that oxysterols can interfere with lipid ordering [16,27]. This, in turn, may have an impact on synaptic vesicle exocytosis [14,31–33]. We investigated whether olesoxime and 5 α Ch3 affect the lipid raft organization at the frog neuromuscular junction by using a marker of rafts (CTxB, which could selectively interact with patches of GM1 ganglioside, predominately located in rafts, [24]) and a specific ligand for postsynaptic nicotinic acetylcholine receptors (α Btx). Fluorescent CTxB-labeled spots were visible in the nerve terminal regions, where they were predominantly localized around the α Btx-staining bands. The intensity of CTxB fluorescence, but not its distribution, was changed in neuromuscular junctions pretreated with olesoxime or 5 α Ch3 for 20 min (Fig. 6A). In the control conditions, the mean intensity of spots was 46.7 ± 1.9 a.u. ($n = 7$ animals, 73 muscle fibers), and after treatment with olesoxime or 5 α Ch3 it increased by $20 \pm 4\%$ ($n = 7$ animals, 75 muscle fibers, $p < 0.05$) or decreased by $28 \pm 5\%$ ($n = 7$ animals, 71 muscle fibers, $p < 0.05$, compared to control) respectively. The opposite changes in the CTxB staining after application of these oxysterols may be caused by an increase or decrease in the “amount” of lipid raft which might, in turn, lead to an “inflow” or “outflow” of GM1-molecules from the membrane raft fraction. According to this scenario, the treatment with oxysterol could create conditions for a strong or a weak interaction of CTxB with GM1-gangliosides of plasma membrane.

3.5.2. Labeling with bodipy-ganglioside GM1

Distribution of fluorescent-labeled ganglioside GM1 fluorescence in the synaptic region somewhat resembled the pattern of CTxB fluorescence (Fig. 6B). Under the control conditions, no changes in the fluorescence were over a 30 min of observation period ($n = 6$ animals). Exposure to olesoxime for 20 min led to an increase the fluorescence in bright spots (by $26 \pm 3\%$, $n = 7$ animals, $p < 0.05$), while ganglioside GM1 fluorescence in the outline of synaptic region was not modified significantly ($p > 0.05$). After treatment with 5 α Ch3 the fluorescence in spots decreased by $30 \pm 4\%$ of the initial value ($n = 8$ animals, $p < 0.05$) without changing in the average intensity of fluorescence in the outline of synaptic region ($p > 0.05$). Herewith, the decrease in fluorescence of spots was associated with spreading of the spot fluorescence. The observed shifts in fluorescence could occur due to aggregation [25] of the bodipy-GM1-molecules into rafts (effect of olesoxime) or their dispersion throughout the synaptic membranes upon raft disruption (effect of 5 α Ch3).

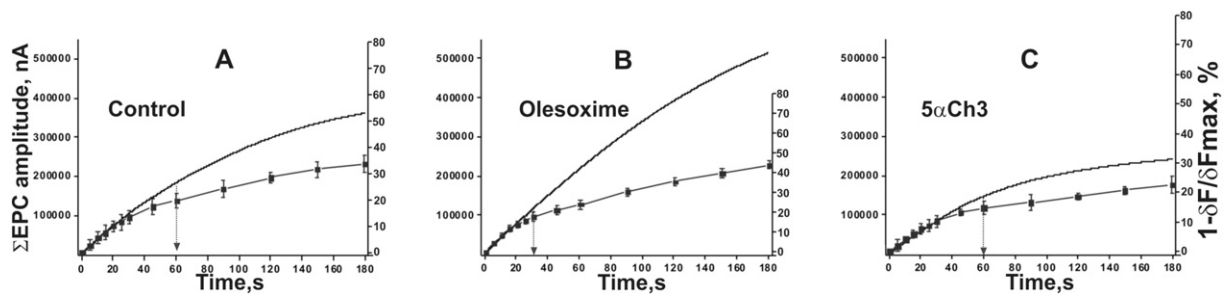


Fig. 5. Estimation of synaptic vesicle recycling time. The inverted FM1–43 destaining curve (from Fig. 4C) was scaled and superimposed on the cumulative amplitude of EPC curve (from Fig. 2D) to achieve a merge into their initial parts. The mean recycling time was estimated as the point of apparent divergence between the curves (noted by an arrow). Olesoxime reduces this time, while 5 α Ch3 has no significant impact.

3.5.3. Time course of 22-NBD-fluorescence

For additional test of the possibility that olesoxime and 5 α Ch3 affect the lipid phase behavior, labeling with 22-NBD-cholesterol was used (Fig. 6C). 22-NBD-cholesterol reacts to phase changes of membrane lipids by enhancing its green fluorescence signal in response to a shift from raft to non-raft fractions [26,27]. In 22-NBD-cholesterol staining neuromuscular preparations, fluorescent bands were observed at the muscle fibers (data not shown), and fluorescence was revealed within the outline of superficial synaptic regions labeled with α Btx. In the last case, 22NBD-cholesterol fluorescence was significantly more extended than of the distribution of Btx signals. Addition of olesoxime caused a decrease of fluorescence in the synaptic region (Fig. 6C): within 20 min of the application, the fluorescence fell to $87.3 \pm 2.0\%$ of the initial baseline ($n = 6$ animals, $p < 0.05$ versus control, $98.9 \pm 1.5\%$, $n = 8$ animals). In contrast, 5 α Ch3 induced an increase of the fluorescence from the synaptic region (up to $110.2 \pm 1.4\%$ after 20 min of the oxysterol treatment, $n = 8$ animals, $p < 0.05$ versus control) (Fig. 6C). The attenuation of 22-NBD-cholesterol fluorescence signal during the application of olesoxime can reflect a formation of liquid-ordered phase (rafts) within the synaptic region. Conversely, the enhancement of the fluorescence in response to 5 α Ch3 application suggests a disruption of the synaptic lipid rafts.

3.5.4. Immunolabeling

To test whether the two oxysterols affect active zone organization, the location of syntaxin 1 (active zone protein) and synaptophysin (synaptic vesicle protein) was investigated using immunofluorescence. Both syntaxin 1 and synaptophysin are highly conserved [1]. Fig. 6D shows immunochemical detection of syntaxin 1 (red channel) and synaptophysin (green channel) in segments of the nerve terminals. The green and red fluorescence in the nerve terminals had a specific punctate pattern of distribution [28]. Both red and green signals were generally co-localized in the control nerve terminals ($n = 6$ animals), but synaptophysin immunolabeling spread over a larger area. Pre-exposure to olesoxime ($n = 6$ animals) or 5 α Ch3 ($n = 6$ animals) did not markedly modify the staining of syntaxin 1 or of synaptophysin and the degree of overlap in their distribution was similar to that in

the control (Fig. 6D). These results suggest no dramatic changes in the spatial organization of active zones.

4. Discussion

4.1. The oxysterols and neuromuscular transmission

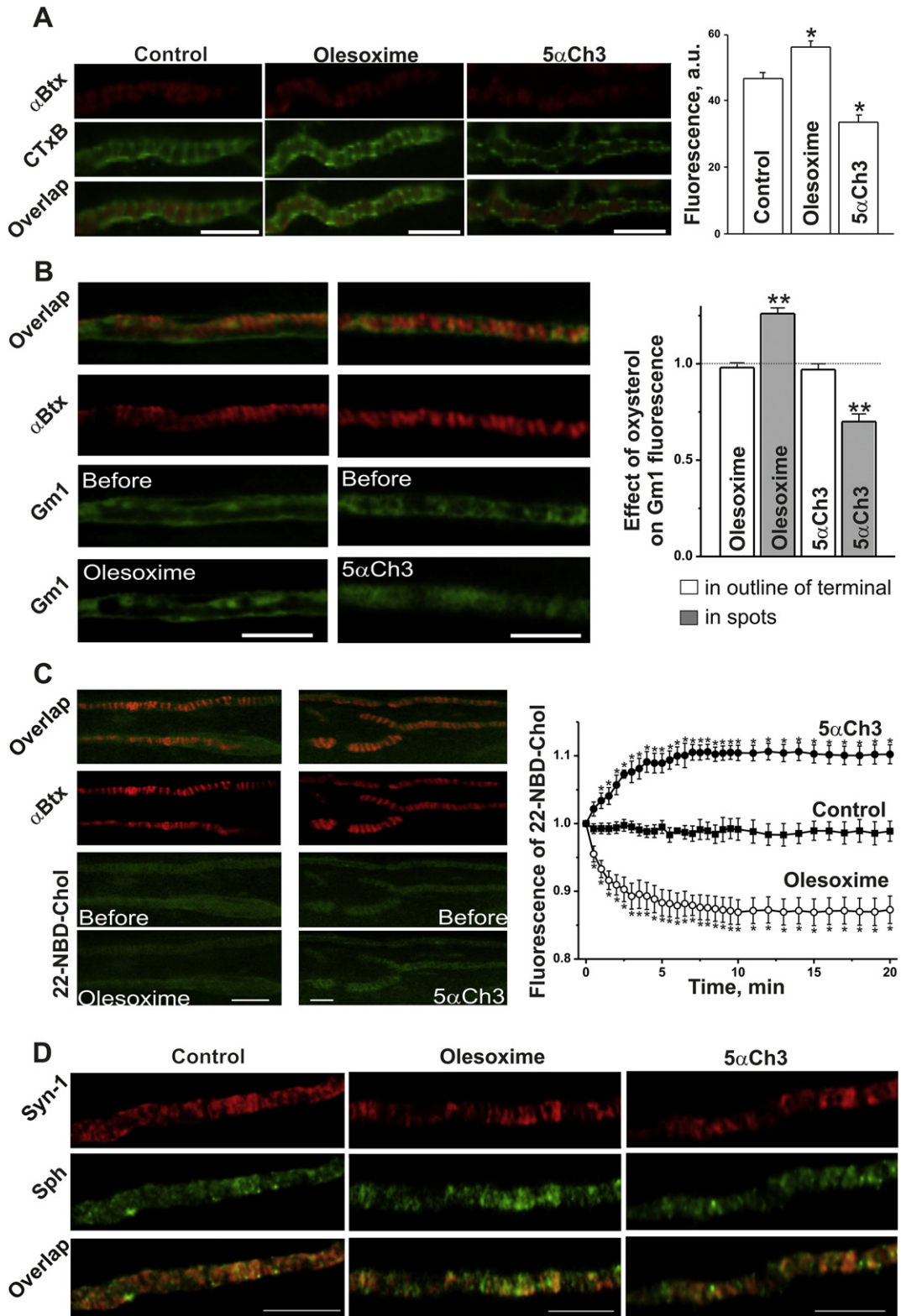
The main findings of the current work are: the discovery of a presynaptic effect of olesoxime, including the description of olesoxime-driven changes in synaptic vesicle cycling, and the disclosure of opposite actions of olesoxime and the structurally related oxysterol, 5 α Ch3. This newly shown biological activity of olesoxime may contribute to the beneficial effects of this neuroprotective molecule in models of neurodegenerative disease and suggests the possibility of the therapeutic use of olesoxime in neuromuscular diseases associated with a lack in neurotransmitter release. Indeed, synaptic activity is thought to impact on development of some neurodegenerative diseases in which synaptic dysfunction is an early sign [34].

Olesoxime has no effect on spontaneous neurotransmitter release but slightly increases evoked release in response to a single stimulus and significantly attenuates the decline in transmitter release during high frequency activity. In the same way, dye unloading during moderate (2 Hz) and high (20 Hz) frequency stimulation occurs faster at olesoxime-pretreated synapses. Eventually, 20 Hz-stimulus trains (lasting 3 min) also cause more release of neurotransmitter (cumulative EPC) and more uptake of dye (loading). This indicates that olesoxime potentiates neuromuscular transmission by increasing both evoked exocytosis and the number of synaptic vesicles involved in cycles of exo-endocytosis. An additional enhancement of neurotransmission during rhythmic activity may result from an increase in the rate of synaptic recycling [1,23,29,30]. Thus, in olesoxime-pretreated synapses, the estimated time of recycling is shorter. Furthermore, the apparent increase in the cumulative EPC amplitude versus the lesser increase in the total dye loading suggests that some of synaptic vesicles take part in neurotransmission several times [22,23,30]. Finally, olesoxime enhances the destaining of FM2–10 dye, previously loaded into synaptic vesicles belonging to recycling pool, which are able to recycle rapidly [30]. Thus, olesoxime promotes neuromuscular transmission by enhancing both

Fig. 6. Impact of the oxysterols on membrane properties at neuromuscular junction. A. The muscles were dual labeled with rhodamine-conjugated α -bungarotoxin (α Btx, red channel) and Alexa488-conjugated cholera toxin subunit B (CTxB, green channel). Left, the labeling in the control and after oxysterol pretreatment. Overlap between the channels is shown in the 3-rd row. Right, average fluorescence of CTxB (in a.u.) from the control muscles and after exposure to olesoxime or 5 α Ch3. The increase and decrease in CTxB fluorescence indicate lipid raft formation or disruption, respectively. B. Double labeling of samples using bodipy-ganglioside GM1 (green, Gm1) and α Btx (red). The fluorescence images (before and 20 min after oxysterol application) are provided on the left. The top image represents overlap between the green and red fluorescence. The measurements of the green fluorescence in outline of synaptic region (light bar) and in bright spots (gray bar) 20 min after exposition to olesoxime or 5 α Ch3 are shown on the right. Y-axis shows the normalized effect of oxysterol (1.0 – is the value before the oxysterol application). No changes in fluorescence were detected for 20 min under control conditions (data not shown). The enhancement or reduction in fluorescence of the spots could be caused by lipid raft organization or disorganization, respectively. C. Left, the fluorescent images of neuromuscular junctions labeled simultaneously with 22-NBD-cholesterol (green) and α Btx before and after treatment (20 min) with olesoxime or 5 α Ch3; the top image represents overlap. Right, changes in fluorescence of 22-NBD-cholesterol in the synaptic region at rest and in response to the application of olesoxime or 5 α Ch3. Oxysterol was added to the bath solution immediately after the moment “0” on the X-axis. The decrease/increase in 22-NBD-fluorescence might reflect the ordering/disordering of lipid membranes in response to olesoxime/5 α Ch3. Y-axis – normalized fluorescence intensity, the initial fluorescence prior to the addition of oxysterol was taken as 1.0. D. Double-immunofluorescent staining of syntaxin 1 (Syn-1, active-zone protein; red) and synaptophysin (Sph, synaptic vesicle protein; green) at control and olesoxime/5 α Ch3-pretreated preparations. The green and red fluorescent images were merged (overlap) to display the relative distribution of syntaxin 1 and synaptophysin. On A, B, C – asterisks denote significant differences (* $p < 0.05$, ** $p < 0.01$). A–D, scale bars – 5 μ m.

evoked exocytosis, and the recycling and recruitment of synaptic vesicles from both recycling and reserve pools to the sites of exocytosis. In principle, it could be useful to enhance synaptic transmission that is impaired as a result of pathological processes. It may well be that some of the neuroprotective effects of olesoxime in disease models of amyotrophic lateral sclerosis, peripheral neuropathies and neurodegenerative pathologies [11,16–19] is linked to changes in the presynaptic vesicle cycle.

Despite their structural similarities, oxysterols can regulate biological processes in a specific manner. For example, 24(S)-hydroxycholesterol selectively enhances glutamate NMDA receptor function [12], whereas 25-hydroxycholesterol is an antagonist of this positive allosteric modulation [35]. In contrast to the neuroprotective activity of olesoxime, the overproduction of 5 α Ch3 in the rare genetic disorder of bile acid synthesis, cerebrotendinous xanthomatosis, is associated with progressive neurological dysfunction and myopathy [15].



5 α Ch3 increased spontaneous exocytosis only slightly, but it significantly decreased evoked release of neurotransmitter. Along the same lines cholesterol depletion by methyl- β -cyclodextrin (M β CD) or inhibition of cholesterol synthesis affects spontaneous and evoked neurotransmitter release in the opposite directions [4,6,8]. Collectively, these results suggest that the changes in cholesterol homeostasis may tilt the balance between spontaneous and evoked release. Moreover, at neuromuscular junctions pretreated with 5 α Ch3, the depression of transmitter release induced by high frequency activity was markedly accelerated, but only 30–40 s after onset of the stimulation. This is consistent with the visible decline in FM1–43 unloading rate starting from ~40 s after the onset of high frequency stimulation. During this period synaptic vesicles belonging to the reserve pool are actively involved in neurotransmission [23,30]. Finally, a train of 3600 stimuli at 20 Hz induced the release of ~1/3 less neurotransmitter and the uptake of ~1/4 less dye than in the control synapses. Therefore, 5 α Ch3 affects synaptic transmission by suppressing both evoked exocytosis and the recruitment of synaptic vesicles from the reserve pool for neurotransmitter release. These results are in good agreement with our recent work, where it has been revealed that 5 α Ch3 can reduce the number of vesicles actively recruited during synaptic transmission at mouse neuromuscular junction [14].

In the initial period (20–30 s) of high frequency stimulation, transmitter release is not dramatically decreased by 5 α Ch3 (although the initial quantum content was reduced, the rate of the EPC amplitude depression was also reduced) and the kinetics of FM1–43 unloading appears similar to control values. In addition, the FM2–10 unloading rate due to exocytosis of synaptic vesicles from the recycling pool is not altered by 5 α Ch3. In summary, there are no significant changes in the recycling pool behavior. In line with this suggestion, the average time of synaptic vesicle recycling remains constant during high frequency stimulation. This time is determined by the rate of exo-endocytosis cycling of synaptic vesicles from the recycling pool [23,30]. Thus, in contrast to the mouse neuromuscular junction, the predominant change in behavior of the synaptic reserve pool is the hallmark of 5 α Ch3 action at the frog neuromuscular junction. This may be linked to the distinctive organization of the recycling pool in frog motor nerve terminals. In the frog, the vesicles in the recycling pool are mobile and their movements are consistent with simple diffusion (like vesicles in photoreceptors, but to a much lesser extent), while vesicles in the reserve pool are immobile (like vesicles in hippocampal terminals) [36]. Vesicular mobility in the mouse motor nerve terminals also has a similar dependence on phosphorylation to that of reserve pool vesicles in the frog [37].

4.2. The oxysterols and membrane properties

In principle, the mechanism of oxysterol action on neuromuscular transmission could be linked with changes in membrane properties and raft-associated signaling. To test the possibility that the oxysterols can affect the properties of synaptic membranes, we used fluorescent lipid raft marker (CTxB), fluorescent-labeled ganglioside GM1 and environment sensitive probe (22-NBD-cholesterol). CTxB targets to GM1 gangliosides predominantly found in the lipid rafts and binds with more affinity to GM1 molecules incorporated into the membranes having a lipid raft-like composition [24]. Bodipy-GM1-ganglioside can partition preferentially into liquid-ordered phase of the living cells mimicking endogenous GM1 [25]. In the membranes of living cells 22-NBD-cholesterol is presumably distributed in the cholesterol-poor phase and its fluorescence increases upon lipid-disordering without any appreciable change in the spectral properties [26,27]. The stainings with CTxB and bodipy-ganglioside GM1 indicate that olesoxime or 5 α Ch3 can increase or decrease the stability of synaptic rafts (liquid-ordered microdomains). Indeed, olesoxime enhances both the CTxB binding to synaptic membranes and the fluorescence of the bodipy-ganglioside GM1 within the spots. Whereas 5 α Ch3 attenuates the labeling of the membranes with CTxB and causes the spreading of the

bodipy-ganglioside GM fluorescence spots along the length of the synaptic region. In addition, these oxysterol changes the 22-NBD-cholesterol fluorescence in opposite directions: olesoxime or 5 α Ch3 leads to a decrease or increase of the dye fluorescence, respectively. This suggests that the action of olesoxime may be related to an expansion of a lipid-ordering and a reduction in a lipid-disordered phase. Accordingly to this scenario, 5 α Ch3 can tilt the lipid phase balance towards a lipid-disordering. These findings are consistent with the observations that olesoxime decreases the fluidity of isolated mitochondrial membranes from striatal cells [17] and the 5 α Ch3 reduces CTxB staining and increases 22-NBD fluorescence in the synaptic membranes of mice neuromuscular junctions [14]. It should be noted that in the preparations treated with olesoxime or 5 α Ch3, the distribution of presynaptic (syntaxin 1 and synaptophysin) and postsynaptic (nicotinic acetylcholine receptors) components is normal, indicating no apparent changes in the structure of frog neuromuscular junctions.

4.3. Putative pathways of the oxysterol action

Many of the proteins involved in the synaptic vesicle cycle have been found in fractions of detergent-resistant membranes, indicating location in lipid rafts [32]. It follows that shifts in lipid raft stability caused by the oxysterols might impact on synaptic vesicle exocytosis and recycling [3–6,13,31–33]. Frequently, lipid raft disruption attenuates evoked neurotransmission, while an increase in raft density should have the opposite effect. Disruption of lipid rafts by cholesterol depletion alters the colocalization of Cav2.1 channels with the proteins of the exocytic machinery and also impairs Ca²⁺ influx in response to depolarization of the isolated rat synaptosomes [38]. At crayfish neuromuscular junctions, high concentration of M β CD (10 mM) blocks evoked transmitter release that is correlated with presynaptic hyperpolarization and failure of action potential propagation [8]. Even lower concentration of M β CD (1 mM) decreases evoked exocytosis and delivery of synaptic vesicle to active zones in the frog and rat neuromuscular junctions [4,5]. In contrast, the spontaneous transmitter release is increased by high level of M β CD in the neuromuscular and central synapses, which can be related to an activation of the signaling enzymes (e.g. protein kinases, calcineurin, NADPH-oxidase) [6,8,39–41]. In hippocampal cultures treated by M β CD or inhibitor of cholesterol biosynthetic pathway, and in the cultures from Niemann–Pick type C1-deficient mice defective in intracellular cholesterol trafficking occur an augmentation of spontaneous neurotransmission, but responses evoked by action potentials and hypertonicity are severely impaired. The last observation suggests that cholesterol removal has a direct effect on evoked exocytosis and retrieval machinery, rather than on voltage-gated Ca²⁺ influx [42]. Cholesterol-enriched microdomains participate in clusterization of syntaxin in the plasmalemma that is important for maintaining the rate of depolarization-induced secretion in the neuroendocrine cells [43]. Some neuromodulators can change the association of synaptic proteins with rafts, whereby affecting the neurotransmitter release. Extracellular α -synuclein, applied to rat neurons in culture or striatal slices, leads to a decrease in plasma membrane cholesterol, resulting in alteration of both the partitioning of Cav2.2 channels (from raft to cholesterol-poor fraction) and neurotransmitter release [44]. After stimulation of synaptosomes from rat brain with bradykinin, protein NCS-1 (neuronal calcium sensor 1) is rapidly recruited to lipid rafts and enhances the activity of Cav2.1 channels which stimulate neurosecretory process [45]. Activation of adenosine A (2A) receptors induces a recruitment of TrkB receptors to lipid rafts and this facilitates the BDNF stimulatory effects on glutamate release from cortical synaptosomes [46]. Besides involvement of rafts in exocytosis, the membrane microdomains may play a pivotal role in synaptic vesicle endocytosis. Given that synaptic vesicles have a high cholesterol and ganglioside GM1 levels [47], that vesicular proteins are found in detergent-resistant membranes [32], vesicular membrane could contain increased levels of lipid rafts. This is in agreement with findings that slight depletion of

vesicular cholesterol impairs synaptic vesicle endocytosis and recycling in neuromuscular and central synapses [4,5,7,48]. Vesicular rafts may be essential for aggregation of exocytosed synaptic vesicle proteins into patches on the presynaptic membrane which facilitates sorting of cargo proteins into the forming vesicles [2,4]. Another potential pathway, by which the changes in raft stability affect synaptic vesicle cycling, could be related to an alteration in signaling through raft-associated autoreceptors that tonically modulate the neurotransmitter release [3]. Thus, we speculate that enhancement of synaptic vesicle exocytosis and recycling induced by olesoxime, at least partially, occurs due to increased lipid raft formation, while the 5 α Ch3-mediated attenuation of exocytosis is dependent on disruption of rafts in the synaptic membranes.

The underlying molecular mechanism of the oxysterol actions remains unclear. Olesoxime and 5 α Ch3 are effective in relatively low concentration. Accordingly, specific binding sites, through which these compounds can affect the membrane properties and/or vesicular cycling, may exist. Conserved family of oxysterol-binding proteins (OSBP) may be involved in the responses to olesoxime and 5 α Ch3. OSBP are implicated in the formation of both membrane contact sites and lateral microdomains, which participate in the control of signaling events [49]. The activity of signaling enzymes (e.g., protein phosphatases and kinases), able to regulate vesicular cycling, could be linked to OSBP. Furthermore, it seems probable that some OSBP can directly interact with synaptic vesicles via vesicular proteins (VAMP, Rab GTPases) or membrane phosphoinositides [14,49,50].

In the contact sites between mitochondria (and endoplasmic reticulum) present a major protein of the outer mitochondrial membrane, voltage-dependent anion channel (VDAC), which can bind with high affinity to olesoxime and participate in mitochondrial cholesterol transport/distribution [51]. Note that VDAC may associate with lipid rafts in the plasma membrane of various cell types (including hippocampal cell and synaptic membranes) and estrogen receptor α , protein kinase A α [11,51,52]. It may be that olesoxime, and the structurally similar 5 α Ch3, modulate synaptic function through a VDAC-related pathway. Bath applications of both oxysterols decrease MitoSox fluorescence in the synaptic region of frog neuromuscular junction, indicative of a reduction of mitochondrial reactive oxygen species (our unpublished observation). Similarly, olesoxime inhibits reactive oxygen species production in adult mouse neurons, probably acting via VDAC as a component of the mitochondrial permeability transition pore [19].

The opposite effects of olesoxime and 5 α Ch3 may be related to their ability to act as agonists or antagonists of an unidentified “receptor”. Further molecular studies are required to identify the oxysterol-targets which are involved in regulating the presynaptic vesicular cycle. The results of such studies might help to improve understanding of how oxysterols regulate synaptic transmission.

Supplementary data to this article can be found online at <http://dx.doi.org/10.1016/j.bbali.2016.04.010>.

Author contributions

All experiments were performed in the laboratory of the Department of Normal Physiology at Kazan State Medical University. M.R.K., G.F. Z., A.R.G., and A.M.P. performed all experiments, data collection and analysis. A.M.P., M.R.K., and A.L.Z. interpreted the results of experiments. A.M.P. designed and wrote the manuscript. The project was directed by A.M.P. All the authors read and approved the final version of the manuscript.

Competing interests

We declare no competing interests.

Transparency document

The Transparency document associated with this article can be found in the online version.

Acknowledgments

We thank Professor Clarke Slater (Newcastle University) for helpful comments on the manuscript. This study was supported by the grant from RFBR #14-04-00094.

References

- [1] T.C. Sudhof, The synaptic vesicle cycle, *Annu. Rev. Neurosci.* 27 (2004) 509–547, <http://dx.doi.org/10.1146/annurev.neuro.26.041002.131412>.
- [2] J.S. Dason, A.J. Smith, L. Marin, M.P. Charlton, Cholesterol and F-actin are required for clustering of recycling synaptic vesicle proteins in the presynaptic plasma membrane, *J. Physiol.* 592 (2014) 621–633.
- [3] A. Giniatullin, A. Petrov, R. Giniatullin, The involvement of P2Y12 receptors, NADPH oxidase, and lipid rafts in the action of extracellular ATP on synaptic transmission at the frog neuromuscular junction, *Neuroscience* 285 (2015) 324–332, <http://dx.doi.org/10.1016/j.neuroscience.2014.11.039>.
- [4] A.M. Petrov, M.R. Kasimov, A.R. Giniatullin, O.I. Tarakanova, A.L. Zefirov, The role of cholesterol in the exo- and endocytosis of synaptic vesicles in frog motor nerve endings, *Neurosci. Behav. Physiol.* 40 (2010) 894–901, <http://dx.doi.org/10.1007/s11055-010-9338-9>.
- [5] A.M. Petrov, N.V. Naumenko, K.V. Uzinskaya, A.R. Giniatullin, A.K. Urazaev, A.L. Zefirov, Increased non-quantal release of acetylcholine after inhibition of endocytosis by methyl- β -cyclodextrin: the role of vesicular acetylcholine transporter, *Neurosci.* 186 (2011) 1–12, <http://dx.doi.org/10.1016/j.neuroscience.2011.04.051>.
- [6] A.M. Petrov, A.A. Yakovleva, A.L. Zefirov, Role of membrane cholesterol in spontaneous exocytosis at frog neuromuscular synapses: ROS calcium interplay, *J. Physiol.* 592 (2014) 4995–5009, <http://dx.doi.org/10.1113/jphysiol.2014.279695>.
- [7] H.Y. Yue, J. Xu, Cholesterol regulates multiple forms of vesicle endocytosis at a mammalian central synapse, *J. Neurochem.* 134 (2015) 247–260.
- [8] O. Zamir, M.P. Charlton, Cholesterol and synaptic transmitter release at crayfish neuromuscular junctions, *J. Physiol.* 571 (2006) 83–99, <http://dx.doi.org/10.1113/jphysiol.2005.098319>.
- [9] B. Malgrange, I. Varela-Nieto, P. de Medina, M.R. Paillasse, Targeting cholesterol homeostasis to fight hearing loss: a new perspective, *Front. Aging Neurosci.* 7 (2015) 3, <http://dx.doi.org/10.3389/fnagi.2015.00003>.
- [10] T.J. Nelson, D.L. Alkon, Oxidation of cholesterol by amyloid precursor protein and beta-amyloid peptide, *J. Biol. Chem.* 280 (2005) 7377–7387.
- [11] T. Bordet, B. Buisson, M. Michaud, C. Drouot, P. Gal e, N.P. Akentieva, A.S. Evers, D.F. Covey, M.A. Ostuni, J.J. Lacap ere, C. Massaad, M. Schumacher, E.M. Steidl, D. Maux, M. Delaage, C.E. Henderson, R.M. Pruss, Identification and characterization of cholest-4-en-3-one, oxime (TRO19622), a novel drug candidate for amyotrophic lateral sclerosis, *J. Pharmacol. Exp. Ther.* 322 (2007) 709–720.
- [12] S.M. Paul, J.J. Doherty, A.J. Robichaud, G.M. Belfort, B.Y. Chow, R.S. Hammond, D.C. Crawford, A.J. Linsenbardt, H.J. Shu, Y. Izumi, S.J. Mennerick, C.F. Zorumski, The major brain cholesterol metabolite 24(S)-hydroxycholesterol is a potent allosteric modulator of N-methyl-D-aspartate receptors, *J. Neurosci.* 33 (2013) 17290–17300, <http://dx.doi.org/10.1523/JNEUROSCI.2619-13.2013>.
- [13] A.M. Petrov, M.R. Kasimov, A.R. Giniatullin, A.L. Zefirov, Effects of oxidation of membrane cholesterol on the vesicle cycle in motor nerve terminals in the frog *Rana ridibunda*, *Neurosci. Behav. Physiol.* 44 (2014) 1020–1030, <http://dx.doi.org/10.1007/s11055-014-0019-y>.
- [14] M.R. Kasimov, A.R. Giniatullin, A.L. Zefirov, A.M. Petrov, Effects of 5 α -cholestan-3-one on the synaptic vesicle cycle at the mouse neuromuscular junction, *Biochim. Biophys. Acta* 1851 (2015) 674–685.
- [15] A.E. DeBarber, Y. Sandler, A.S. Pappu, L.S. Merckens, P.B. Duell, S.R. Lear, S.K. Erickson, R.D. Steiner, Profiling sterols in cerebrotendinous xanthomatosis: utility of Girard derivatization and high resolution exact mass LC-ESI-MS(n) analysis, *J. Chromatogr. B Anal. Technol. Biomed. Life Sci.* 879 (2011) 1384–1392, <http://dx.doi.org/10.1016/j.jchromb.2010.11.019>.
- [16] A. Kaczmarek, S. Schneider, B. Wirth, M. Riessland, Investigational therapies for the treatment of spinal muscular atrophy, *Expert Opin. Investig. Drugs* 24 (2015) 867–881, <http://dx.doi.org/10.1517/13543784.2015.1038341>.
- [17] J. Eckmann, L.E. Clemens, S.H. Eckert, S. Hagl, L. Yu-Taeger, T. Bordet, R.M. Pruss, W.E. Muller, K. Leuner, H.P. Nguyen, G.P. Eckert, Mitochondrial membrane fluidity is consistently increased in different models of Huntington disease: restorative effects of olesoxime, *Mol. Neurobiol.* 50 (2014) 107–118, <http://dx.doi.org/10.1007/s12035-014-8663-3>.
- [18] C. Gouarn e, J. Tracz, M.G. Paoli, V. Deluca, M. Seimandi, G. Tardif, M. Xilouri, L. Stefanis, T. Bordet, R.M. Pruss, Protective role of olesoxime against wild type alpha-synuclein-induced toxicity in human neuronally differentiated SHSY-5Y cells, *Br. J. Pharmacol.* 172 (2014) 235–245, <http://dx.doi.org/10.1111/bph.12939>.
- [19] L.J. Martin, N.A. Adams, Y. Pan, A. Price, M. Wong, The mitochondrial permeability transition pore regulates nitric oxide-mediated apoptosis of neurons induced by target deprivation, *J. Neurosci.* 31 (2011) 359–370, <http://dx.doi.org/10.1523/JNEUROSCI.2225-10.2011>.

- [20] M.I. Glavinović, Voltage clamping of unparalysed cut rat diaphragm for study of transmitter release, *J. Physiol.* 290 (1979) 467–480.
- [21] J.J. Lambert, N.N. Durant, L.S. Reynolds, R.L. Volle, E.G. Henderson, Characterization of end-plate conductance in transected frog muscle: modification by drugs, *J. Pharmacol. Exp. Ther.* 216 (1981) 62–69.
- [22] W.J. Betz, G.S. Bewick, Optical monitoring of transmitter release and synaptic vesicle recycling at the frog neuromuscular junction, *J. Physiol.* 460 (1993) 287–309.
- [23] A.M. Petrov, A.R. Giniatullin, G.F. Sitdikova, A.L. Zefirov, The role of cGMP-dependent signaling pathway in synaptic vesicle cycle at the frog motor nerve terminals, *J. Neurosci.* 28 (2008) 13216–13222, <http://dx.doi.org/10.1523/JNEUROSCI.2947-08.2008>.
- [24] G. Margheri, R. D'Agostino, S. Trigari, S. Sottini, M. Del Rosso, The β -subunit of cholera toxin has a high affinity for ganglioside GM1 embedded into solid supported lipid membranes with a lipid raft-like composition, *Lipids* 49 (2014) 203–206, <http://dx.doi.org/10.1007/s11745-013-3845-8>.
- [25] N. Ichikawa, K. Iwabuchi, H. Kurihara, K. Ishii, T. Kobayashi, T. Sasaki, N. Hattori, Y. Mizuno, K. Hozumi, Y. Yamada, E. Arikawa-Hirasawa, Binding of laminin-1 to monosialoganglioside GM1 in lipid rafts is crucial for neurite outgrowth, *J. Cell Sci.* 122 (2009) 289–299, <http://dx.doi.org/10.1242/jcs.030338>.
- [26] L.M. Loura, A. Fedorov, M. Prieto, Exclusion of a cholesterol analog from the cholesterol-rich phase in model membranes, *Biochim. Biophys. Acta* 1511 (2001) 236–243, [http://dx.doi.org/10.1016/S0005-2736\(01\)00269-3](http://dx.doi.org/10.1016/S0005-2736(01)00269-3).
- [27] P. Ostašev, J. Sýkora, J. Brejchová, A. Olžýřnska, M. Hof, P. Svoboda, FLIM studies of 22- and 25-NBD-cholesterol in living HEK293 cells: plasma membrane change induced by cholesterol depletion, *Chem. Phys. Lipids* 167–168 (2013) 62–69, <http://dx.doi.org/10.1016/j.chemphyslip.2013.02.006>.
- [28] C.R. Slater, The functional organization of motor nerve terminals, *Prog. Neurobiol.* 134 (2015) 55–103, <http://dx.doi.org/10.1016/j.pneurobio.2015.09.004> (Epub 2015 Oct 9. Review).
- [29] B. Reid, C.R. Slater, G.S. Bewick, Synaptic vesicle dynamics in rat fast and slow motor nerve terminals, *J. Neurosci.* 19 (1999) 2511–2521.
- [30] D.A. Richards, C. Guatimosim, W.J. Betz, Two endocytic recycling routes selectively fill two vesicle pools in frog motor nerve terminals, *Neuron* 27 (2000) 551–559.
- [31] B.N. Olsen, P.H. Schlesinger, D.S. Ory, N.A. Baker, Side-chain oxysterols: from cells to membranes to molecules, *Biochim. Biophys. Acta* 1818 (2012) 330–336, <http://dx.doi.org/10.1016/j.bbame.2011.06.014>.
- [32] C. Gil, R. Cubí, J. Blasi, J. Aguilera, Synaptic proteins associate with a sub-set of lipid rafts when isolated from nerve endings at physiological temperature, *Biochem. Biophys. Res. Commun.* 348 (2006) 1334–1342.
- [33] T. Lang, SNARE proteins and 'membrane rafts', *J. Physiol.* 585 (2007) 693–698.
- [34] R. Brown, A. Hynes-Allen, A.J. Swan, K.N. Dissanayake, T.H. Gillingwater, R.R. Ribchester, Activity-dependent degeneration of axotomized neuromuscular synapses in Wld S mice, *Neurosci.* 290 (2015) 300–320, <http://dx.doi.org/10.1016/j.neuroscience.2015.01.018>.
- [35] A.J. Linsenbardt, A. Taylor, C.M. Emnett, J.J. Doherty, K. Krishnan, D.F. Covey, S.M. Paul, C.F. Zorumski, S. Mennerick, Different oxysterols have opposing actions at N-methyl-D-aspartate receptors, *Neuropharmacology* 85 (2014) 232–242, <http://dx.doi.org/10.1016/j.neuropharm.2014.05.027>.
- [36] M.A. Gaffield, S.O. Rizzoli, W.J. Betz, Mobility of synaptic vesicles in different pools in resting and stimulated frog motor nerve terminals, *Neuron* 51 (2006) 317–325.
- [37] M.A. Gaffield, W.J. Betz, Synaptic vesicle mobility in mouse motor nerve terminals with and without synapsin, *J. Neurosci.* 27 (2007) 13691–13700.
- [38] E. Taverna, E. Saba, J. Rowe, M. Francolini, F. Clementi, P. Rosa, Role of lipid microdomains in P/Q-type calcium channel (Cav2.1) clustering and function in presynaptic membranes, *J. Biol. Chem.* 279 (2004) 5127–5134, <http://dx.doi.org/10.1074/jbc.M308798200>.
- [39] A.M. Petrov, G.F. Zakyrganova, A.A. Yakovleva, A.L. Zefirov, Inhibition of protein kinase C affects on mode of synaptic vesicle exocytosis due to cholesterol depletion, *Biochem. Biophys. Res. Commun.* 456 (2015) 145–150, <http://dx.doi.org/10.1016/j.bbrc.2014.11.049>.
- [40] A.J. Smith, S. Sugita, M.P. Charlton, Cholesterol-dependent kinase activity regulates transmitter release from cerebellar synapses, *J. Neurosci.* 30 (2010) 6116–6121, <http://dx.doi.org/10.1523/JNEUROSCI.0170-10.2010>.
- [41] G. Teixeira, L.B. Vieira, M.V. Gomez, C. Guatimosim, Cholesterol as a key player in the balance of evoked and spontaneous glutamate release in rat brain cortical synaptosomes, *Neurochem. Int.* 61 (2012) 1151–1159, <http://dx.doi.org/10.1016/j.neuint.2012.08.008>.
- [42] C.R. Wasser, M. Ertunc, X. Liu, E.T. Kavalali, Cholesterol-dependent balance between evoked and spontaneous synaptic vesicle recycling, *J. Physiol.* 579 (2007) 413–429, <http://dx.doi.org/10.1113/jphysiol.2006.123133>.
- [43] T. Lang, D. Bruns, D. Wenzel, D. Riedel, P. Holroyd, C. Thiele, R. Jahn, SNAREs are concentrated in cholesterol-dependent clusters that define docking and fusion sites for exocytosis, *EMBO J.* 20 (2001) 2202–2213, <http://dx.doi.org/10.1093/emboj/20.9.2202>.
- [44] G. Ronzitti, G. Bucci, M. Emanuele, D. Leo, T.D. Sotnikova, L.V. Mus, C.H. Soubbrane, M.L. Dallas, A. Thalhammer, L.A. Cingolani, S. Mochida, R.R. Gainetdinov, G.J. Stephens, E. Chierigatti, Exogenous α -synuclein decreases raft partitioning of Cav2.2 channels inducing dopamine release, *J. Neurosci.* 34 (2014) 10603–10615, <http://dx.doi.org/10.1523/JNEUROSCI.060814.2014>.
- [45] E. Taverna, E. Saba, A. Linetti, R. Longhi, A. Jeromin, M. Righi, F. Clementi, P. Rosa, Localization of synaptic proteins involved in neurosecretion in different membrane microdomains, *J. Neurochem.* 100 (2007) 664–677, <http://dx.doi.org/10.1111/j.1471-4159.2006.04225.x>.
- [46] N. Assaife-Lopes, V.C. Sousa, D.B. Pereira, J.A. Ribeiro, A.M. Sebastião, Regulation of TrkB receptor translocation to lipid rafts by adenosine A(2A) receptors and its functional implications for BDNF-induced regulation of synaptic plasticity, *Purinergic Signal.* 10 (2014) 251–267, <http://dx.doi.org/10.1007/s11302-013-9389-9>.
- [47] S. Takamori, M. Holt, K. Stenius, E.A. Lemke, M. Grønborg, D. Riedel, H. Urlaub, S. Schenck, B. Brügger, P. Ringler, S.A. Müller, B. Rammner, F. Gräter, J.S. Hub, B.L. De Groot, G. Mieskes, Y. Moriyama, J. Klingauf, H. Grubmüller, J. Heuser, F. Wieland, R. Jahn, Molecular anatomy of a trafficking organelle, *Cell* 127 (2006) 831–846.
- [48] J.S. Dason, A.J. Smith, L. Marin, M.P. Charlton, Vesicular sterols are essential for synaptic vesicle cycling, *J. Neurosci.* 30 (2010) 15856–15865, <http://dx.doi.org/10.1523/JNEUROSCI.4132-10.2010>.
- [49] H. Kentala, M. Weber-Boyvatt, V.M. Olkkonen, OSBP-related protein family: mediators of lipid transport and signaling at membrane contact sites, *Int. Rev. Cell Mol. Biol.* 321 (2016) 299–340, <http://dx.doi.org/10.1016/bs.ircmb.2015.09.006>.
- [50] M. Johansson, M. Lehto, K. Tanhuanpää, T.L. Cover, V.M. Olkkonen, The oxysterol-binding protein homologue ORP1L interacts with Rab7 and alters functional properties of late endocytic compartments, *Mol. Biol. Cell* 16 (2005) 5480–5492, <http://dx.doi.org/10.1091/mbc.E05-03-0189>.
- [51] C. Martel, Z. Wang, C. Brenner, VDAC phosphorylation, a lipid sensor influencing the cell fate, *Mitochondrion* 19 (2014) 69–77, <http://dx.doi.org/10.1016/j.mito.2014.07.009> (Pt A).
- [52] R. Marin, C.M. Ramírez, M. González, E. González-Muñoz, A. Zorzano, M. Camps, R. Alonso, M. Díaz, Voltage-dependent anion channel (VDAC) participates in amyloid beta-induced toxicity and interacts with plasma membrane estrogen receptor alpha in septal and hippocampal neurons, *Mol. Membr. Biol.* 24 (2007) 148–160.